Desalination and Water Treatment
www.deswater.com

doi: 10.1080/19443994.2016.1159252

57 (2016) 25773–25782
November

Taylor & Francis
Taylor & Francis Group

Interaction of Pb (II) and Cd (II) with *Arthrobacter protophormiae* biomass: mechanism and characterization

Yu-shan Wan*, Yan-qiu Chen, Li-Hang

Department of Environmental and Safety Engineering, Changzhou University, Changzhou, Jiangsu 213164, P.R. China, Tel./Fax: +86 519 86330086; emails: wanyushan@126.com (Y.-s. Wan), 1063446887@qq.com (Y.-q. Chen), 1091268023@qq.com (Li-Hang)

Received 23 September 2015; Accepted 30 January 2016

ABSTRACT

The interactions of Pb(II) and Cd(II) with *Arthrobacter protophormiae* biomass (a life biomass) were investigated by environmental scanning electron microscopy coupled with energy dispersive X-ray (SEM-EDX) and Fourier transform infrared spectrometer (FTIR) analysis. Atomic force microscopy (AFM) used in the tapping mode elucidated the morphological changes in bacterial cells following both metals binding. The effect of initial metal concentrations (0.04–0.3 mmol/L) on the solution pH variation and metal uptake was investigated at the constant biomass concentration of 0.5 g/L and 25°C. For Cd(II), a shift in the medium pH from 5.0 to a final value c.a. 7.3 (43 h) occurred at the initial concentration of 0.04 mmol/L. A similar pH profile for Pb(II) was observed. The amount of Pb(II) sorbed increased during the first 7 h and thereafter remained nearly constant, whereas the amount of Cd(II) decreased gradually during the 7–43 h. The involvement of cellular phosphate and carboxyl groups in Cd(II) binding was ascertained by FTIR spectroscopy and SEM-EDX analysis. AFM analysis revealed the morphological distortion of the *A. protophormiae* cell after metal uptake. The results suggest different interaction mechanisms for each cation. Pb (II) was removed by both metal adsorption and precipitation, due to the pH shift that occurred during the process, while Cd(II) removal showed to be completely dependent of this pH shift.

Keywords: A. protophormiae biomass; Pb(II); Cd(II); Mechanism; AFM

1. Introduction

Environmental contamination by toxic metals is of growing concern because of the health risks for humans and animals. Presently, considerable attention has been given to the methods for their removal from industrial wastewaters [1–3]. Major process currently being suggested or employed for the removal of toxic metals, include precipitation, cementation, ion exchange, membrane separation, solvent extraction, adsorption [4–6]. A detailed discussion on the advantages and disadvantages of all processes is presented by Rao et al. [4].

Recent attention has concentrated on biotechnological potential in metal removal processes [7]. Bacterial biomass represents an efficient and potential class of biosorbents for the removal of metal ions [8]. Morsy et al. [9] investigated the isotherm and kinetics of Cd (II) and Zn(II) by *nostoc commune* and obtained

*Corresponding author.

promising results. Murugavelh and Mohanty [10] demonstrated that live and active *Phanerochaete chrysosporium* biomass has excellent hexavalent chromium removal capability. Seh-Bardan et al. [11] suggested that *A. fumigatus* has a potential to be used in remediation of heavy metal contaminated sites. Alam and Ahmad [12] used four bacterial isolates (*Stenotrophomonas maltophilia*, *Exiguobacterium* sp., *Pantoea* sp., and *Aeromonas* sp.) to efficiently remove hexavalent chromium from aqueous solution. Jabasingh and Pavithra [13] employed the Box–Behnken design to optimize the biosorption of chromium (Cr^{6+}) by *Mucor racemosus*.

Micro-organisms accumulate heavy metal ions by a number of different processes such as uptake by transport, biosorption to cell walls, and entrapment in extracellular capsules, precipitation, cation exchange, and oxidation–reduction reactions [14,15]. Metal sequestering by different parts of the cell can occur via complexation, coordination, chelation of metals, ion exchange, adsorption, inorganic microprecipitation and/or a combination of the above mechanisms.

The *Arthrobacter protophormiae* strain used was isolated from marine sediment. In this study, we initiated investigations to examine the removal mechanisms for Pb(II) and Cd(II) with *A. protophormiae* biomass. The objectives of the present research were to study: (1) the influence of pH shift during the metal biosorption process on adsorption capacity was evaluated; (2) the mechanism of metal–bacteria interaction has further been elucidated by employing several analytical techniques such as Fourier transform infrared spectroscopy (FTIR), environmental scanning electron microscopy/energy dispersive X-ray analysis (SEM-EDX), and atomic force microscopy (AFM).

2. Materials and methods

2.1. Preparation of biomass

The *A. protophormiae* strain (Gram positive) (characterized by 16S rDNA technology) was isolated from marine sediment. Inocula from fresh slant were used to initiate preculture at 25˚C. At the late logarithmic phase of growth, inocula of 1 mL were transferred and allowed to grow in 50 ml volume of the growth culture medium which contained beef extract (1 g/L), peptone (5 g/L), and pH 7.6–7.8. For agar plates, 15 g of agar per liter was added before autoclaving.

The cells from the late-exponential growth phase were harvested by centrifugation (10,000× *g*, 10 min) at room temperature and washed three times with deionized water in the absence of metabolizable substrate. The biomass was freeze-dried and then stored at 4˚C for subsequent experiments.

2.2. Determination of point of zero charge

The point of zero charge (pH_{PZC}) of the biomass was determined by the solid addition method [16]. To a series of 100-mL conical flasks, 45 mL of KNO_3 solution of known strength was transferred. The pH_0 values of the solution were roughly adjusted from 2 to 12 by adding either 0.1 mol/L HNO_3 or NaOH. The total volume of the solution in each flask was made exactly to 50 mL by adding the KNO_3 solution of the same strength. The pH of the solutions was then accurately noted, and 0.1 g of biomass was added to each flask, which were securely capped immediately. The suspensions were then manually shaken and allowed to equilibrate for 48 h with intermittent manual shaking. The pH values of the supernatant liquid were noted. The difference between the initial (pH_0) and final pH (pH_f) values ($pH_0 - pH_f$) was plotted against the pH_0. The point of intersection of the resulting curve at which pH was the pHzpc. The procedure was repeated for different concentrations (0.01 and 0.1 mol/L) of KNO_3.

The pH_{PZC} of the biomass was determined to be around 2.8, which is identical to the ZPC of the cell wall of a gram-positive bacterium [17]. At solution $pH > pH_{PZC}$, negatively charged sites predominate on the surface of biomass and thus favor metal ions adsorption.

2.3. Characterization by SEM-EDX, FTIR, and AFM

Metal-free control and metal-loaded biomass were used for energy dispersive X-ray microanalysis using a QUANTAX microanalytical system (Bruker, Germany) attached with FEI Quanta 250 environmental scanning electron microscope (USA) (SEM-EDX).

Biomass before and after exposure to both metal ions was also used for FTIR spectroscopic analysis. The infrared spectra were recorded within the range 400–4,000 cm^{-1} in a Tensor 27 FTIR Spectrometer (Bruke, Germany).

A Dimension ICON atomic force microscope (AFM, Bruker, Germany) was used to record AFM images of the cell before and after exposure to both metal ions. Cells were imaged using Silicon nitride (Si_3N_4) cantilevers (OTESPA, Bruker) with a spring constant of 70 N/m at a scan speed of 300 kHz in air.

The muscovite was prepared by carefully cutting several less than 10 × 10 mm pieces from a larger sheet using a pair of scissors or a scalpel. Great care was taken to avoid disturbing or scratching the center

region of the flake where the AFM tip eventually "touches down". AFM imaging was performed using the tapping mode, where, the tip makes intermittent contact with the sample as the tip is oscillated near its resonance frequency. The advantages of the tapping mode are that the sample is less likely to be damaged by the tip and that lateral forces are greatly reduced. Despite these advantages, there are very few reports on application of this technique in investigating bacterial metal sequestration processes [18].

2.4. Release of cellular metal ions (Na^+, Ca^{2+}, Mg^{2+})

The experimental method used in this study was based on the technique suggested by Suh et al. [14]. The experiments were carried out using 100 ml of micro-organism suspension (0.5 g/L) in 250-ml conical flasks in a rotary-shake incubator at 25℃ (150 rpm). The experiments were repeated by instilling Pb $(NO_3)_2$ or Cd $(NO_3)_2$. The concentration was 0.15 mmol/L for Pb(II) and Cd(II), respectively. The initial pH was adjusted to be 5.0 for comparison. Samples were taken at appropriate time points and centrifuged immediately. The Na^+, Ca^{2+}, and Mg^{2+} concentrations in the supernatant were measured by TAS-990 atomic absorption spectrophotometer (AAS, Beijing Puxi Scientific Instrumental Factory, China).

2.5. Adsorption experiments

The stock solution (1,000 mg/L) was prepared by dissolving a known quantity of metal salt ($Pb(NO_3)_2$ or $Cd(NO_3)_2$, respectively) in deionized water. The pH was adjusted with HNO_3 using a PHS-3C pH meter (Jiangsu Jiangfen Instrumental Factory, China) using a combined glass electrode.

To investigate the effect of initial metal ion concentration on the solution pH, the initial concentrations varied from 0.04 to 0.3 mmol/L at the constant biomass concentration of 0.5 g/L and 25℃ (150 rpm). After shaking, the solution samples were withdrawn at suitable time intervals. Temperature control was provided by a water bath shaker unit.

The biomass was removed by centrifugation and the supernatant was analyzed for metal concentration and determined for solution pH value, respectively. The residual metal concentration was determined using TAS-990 atomic absorption spectrophotometer. The pH value was measured by a pH meter. All experiments were performed in triplicate and an average value was obtained.

All chemical reagents used in this study were analytical grade or better. All glassware was washed with 1 mol/L HNO_3 and rinsed thoroughly with deionized water prior to use. Solutions were made with deionized water purified by passage through a milli-Q water system. Controls were comprised of adsorbent in deionized water blank and adsorbent-free metal ions solutions.

2.6. Data analysis

The amount of metal sorbed by the biomass (q_t, mmol/g) was calculated as follows:

$$q_t = \frac{V(C_0 - C_t)}{m} \quad (1)$$

where V is the solution volume (L), m is the amount of sorbent (g), and C_0 and C_t (mmol/L) are the initial and equilibrium metal concentrations, respectively.

3. Results and discussion

3.1. Speciation of aqueous metal ions

The speciation of metal ions in an aqueous solution significantly influences their interaction with a solid adsorbent. In this study, the metal solutions applied were prepared from nitrate compounds. The speciation distributions of both Pb(II) and Cd(II) at different total concentrations versus pH are presented in Fig. 1. The speciation plots were obtained by the Medusa computer program software developed by the Royal Institute of Technology, Sweden. It is found that at pH < 6, Pb(II) species are present totally in ionic states at the total concentration of 4×10^{-5} mol/L. With increasing pH, Pb^{2+} species starts to hydrolyze at pH > 6.2 and entirely precipitate into $Pb(OH)_2$, whereas formation of $Cd(OH)_2$ starts at a higher pH value (c.a. 9.0). With an increase in the total concentration of metal ions, formation of hydroxide precipitates starts at a relatively low pH (5.9 for $Pb(OH)_2$ and 8.5 for $Cd(OH)_2$, respectively).

3.2. Time profile of solution pH

To investigate the effect of initial metal ion concentration on the solution pH variation, the initial concentrations varied from 0.04 to 0.3 mmol/L at the constant biomass concentration of 0.5 g/L. As shown in Fig. 2(a), as Cd(II) adsorption proceeded, solution pH value concomitantly varied. The solution pH markedly increased from 5.0 to 6.7 during the first 5 h, then slightly decreased (5–7 h), and then slowly again

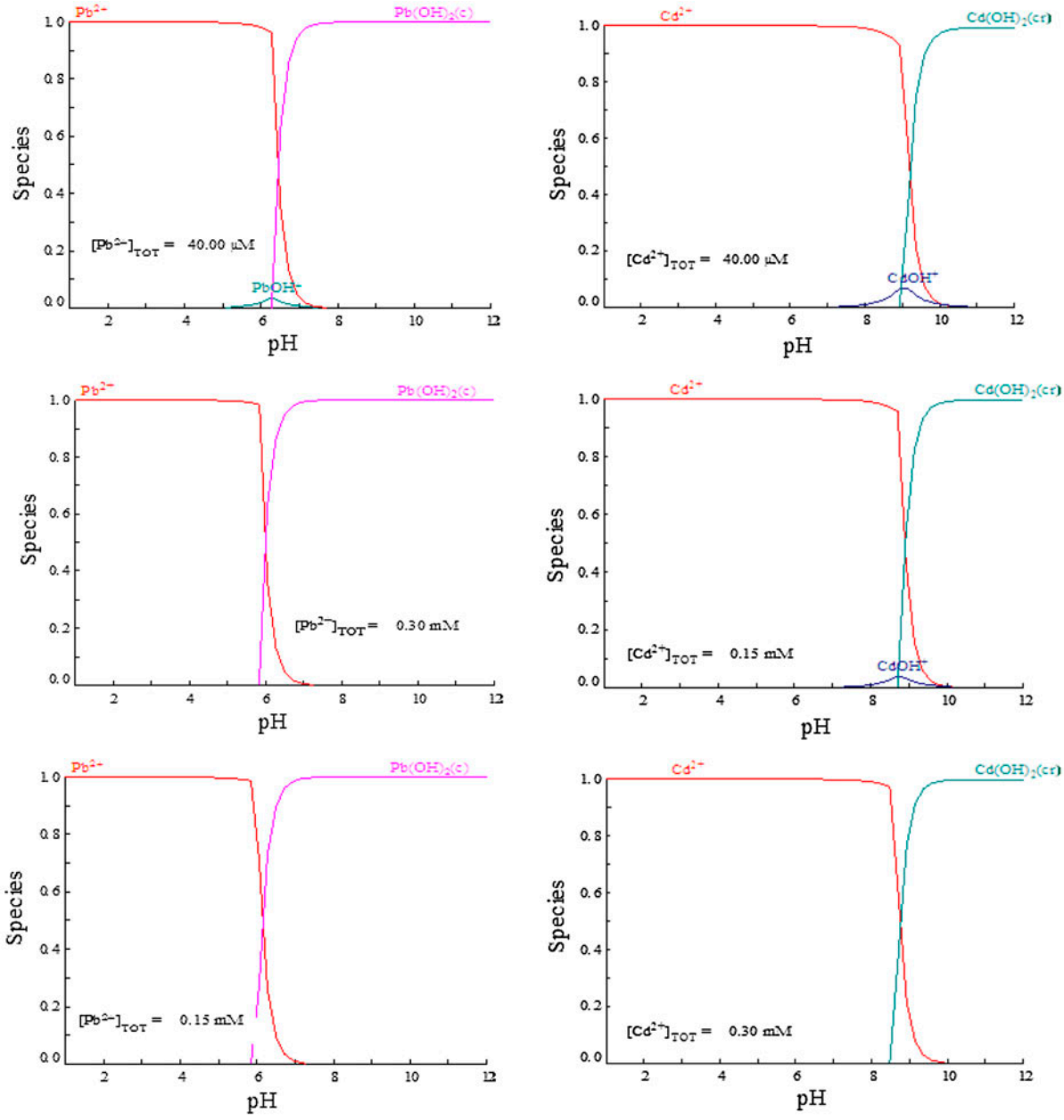

Fig. 1. Species fraction diagrams vs. pH. The speciation plots were obtained by the Medusa computer program software developed by the Royal Institute of Technology, Sweden.

increased to 7.3 at 43 h at the initial concentration of 0.04 mmol/L.

The effect of initial Cd(II) concentration on the solution pH variation is also shown in Fig. 2(a). As expected, with an increase in the initial Cd(II) concentration, the pH variation decreased. This phenomenon was ascribed to a decrease in H^+ uptake or an increase in H^+ release from the biomass. Similar results were obtained by Chen and Wang [19].

A similar pH profile was observed for Pb(II) (Fig. 2(b)). For three runs, solution pH increased sharply to a final value in the 7.6–7.8 range. This phenomenon has already been observed and reported for several other studies of metal biosorption by microbial biomass and reflects an intrinsic ability of the microbial biomass to shift the solution pH toward a favorable value, usually closer to neutrality [20]. Marques et al. [21] also reported that the measured pH shift

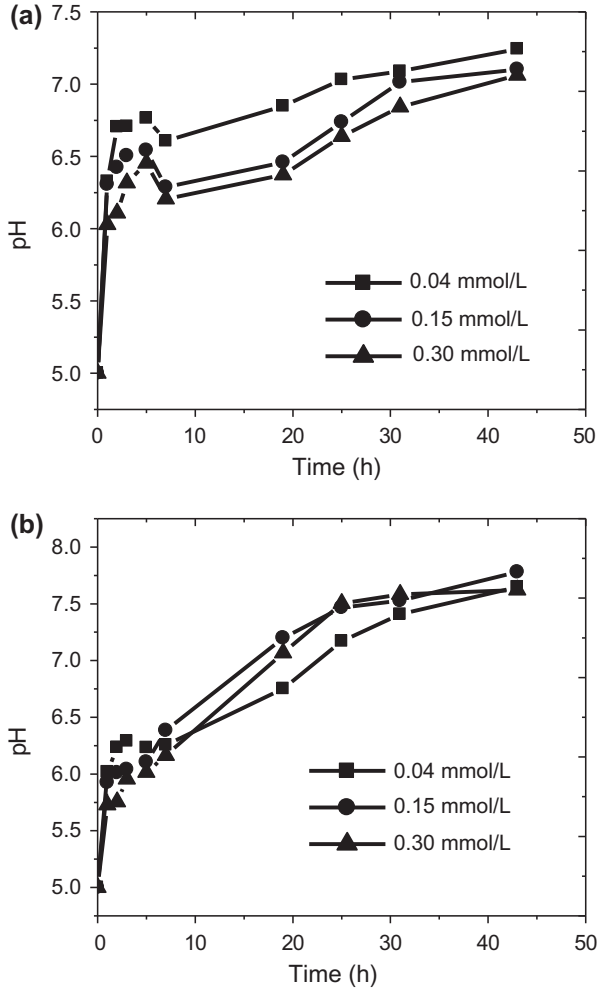

Fig. 2. Time course of pH variation (a) Cd(II) and (b) Pb (II) (initial pH 5.0, adsorbent concentration 0.5 g/L, reaction temperature 25℃).

was not related to the metal uptake but was brought about by the biomass itself, even in the absence of metal. The transfer of this biomass to a low-salt medium apparently brings about osmotic unbalance, which leads to a spontaneous H^+ uptake.

3.3. Time profile of release of cellular metal ions (Na^+, Ca^{2+}, Mg^{2+})

Fig. 3 shows the typical time course in release of cellular metal ions. In the absence of metal ions (Pb(II) and Cd(II), Fig. 3(a)), the released amount of Na^+ sharply increased during the 7 h, thereafter it maintained nearly constant. On the other hand, Ca^{2+} and Mg^{2+} released continuously but their levels were much less

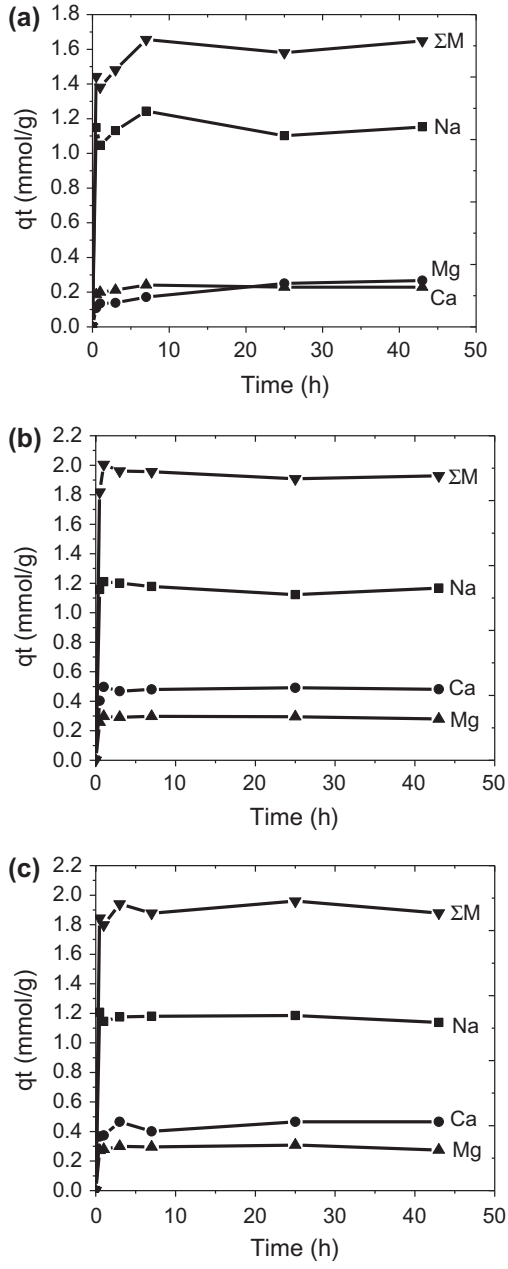

Fig. 3. Time course of release of cellular metal ions (Na^+, Ca^{2+}, Mg^{2+}) ((a) free of Cd(II) and Pb(II), (b) Pb(II) concentration = 0.15 mmol/L, and (c) Cd(II) conentration = 0.15 mmol/L) (initial pH 5.0, adsorbent concentration 0.5 g/L, reaction temperature 25℃). $\sum M$ = sum of amount of Na^+, Ca^{2+}, and Mg^{2+}.

than Na^+. This phenomenon was presumably attributed to the H^+ uptake [21,22]. The presence of Pb(II) (Fig. 3(b)) or Cd(II) (Fig. 3(c)) in the medium promoted the release of Ca^{2+} but had a small influence on the release of Na^+ and Mg^{2+}.

3.4. Time profile of metal uptake

Fig. 4 shows the effect of metal initial concentration on metal adsorption. At the initial concentration of 0.04 mmol/L, Cd(II) uptake reached its highest value (0.7 mmol/g) at 7 h, and then decreased gradually with time (0.53 mmol/g at 43 h) (Fig. 4(a)). Moreover, with an increase in the initial metal ion concentration, the Cd(II) uptake increased.

Compared to that of Cd(II), a very different uptake profile for Pb(II) was observed (Fig. 4(b)). At the initial concentration of 0.04 mmol/L, the Pb(II) uptake reached to its maximal level (0.74 mmol/g) at 7 h, then maintained almost constant.

The discrepancy in Cd(II) and Pb(II) removal may be attributed to their different adsorption mechanisms. Biosorption is a complex phenomenon. Metal sequestering by different parts of the cell can occur via complexation, coordination, chelation of metals, ion exchange, adsorption, inorganic microprecipitation, and/or a combination of the above mechanisms. Each one of the above mechanisms depends on a number of factors which can be classified into three categories: (1) micro-organism(s) characteristics; (2) physicochemical characteristics of the targeted metals; and (3) micro-environmental characteristics of the solution such as the solution pH and composition [20].

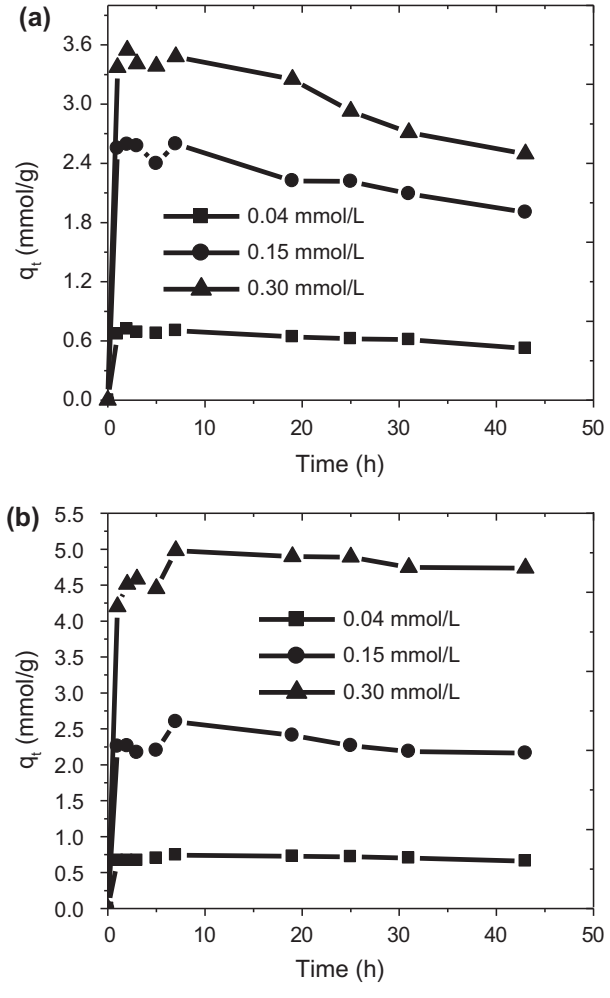

Fig. 4. Time course of metal ions uptake: (a) Cd(II) and (b) Pb(II) (initial pH 5.0, adsorbent concentration 0.5 g/L, reaction temperature 25°C).

In the present system, Cd(II) species are present totally in ionic states at pH < 9 (see Fig. 1). It is believed that Cd(II) removal was principally ascribed to adsorption on the surface of the biomass during the first 7 h. Thereafter, as solution pH value increased further, the higher concentrations of H^+ ions accumulated on the biomass which competed with the Cd(II) for adsorption sites, thus leading to less Cd(II) uptake.

This was not the case for Pb(II). As Pb(II) adsorption proceeded, solution pH value increased dramatically and then exceeded the "optimum" value (6.2, 5.9, 5.9 for initial Pb(II) concentrations of 0.04, 0.15, and 0.3 mmol/L, respectively, see Fig. 1), thus leading to the formation of lead hydroxide precipitate. Pb(II) adsorption occurred according to Eq. (2) and finally achieved a chemical balance.

$$Pb(OH)_2 + MX \longrightarrow PbX + 2(OH^-) + M(Na^+, Ca^{2+}, Mg^{2+}) \quad (2)$$

where X represents the biomass surface ligand (functional groups).

With an increase in pH and amount of cellular metal ions (Na^+, Ca^{2+}, Mg^{2+}), this equilibrium shifts to the left, leading to a decrease in Pb(II) uptake and a rise in Pb $(OH)_2$ precipitates.

The results mentioned above suggest different removal mechanisms for each cation. Pb(II) was removed by both metal adsorption and precipitation, due to the pH shift that occurred during the process, while Cd(II) removal showed to be completely dependent of this pH shift.

3.5. Surface analysis

3.5.1. FTIR

In gram-positive bacteria, the carboxylate and phosphate groups are primarily associated with the peptidoglycan; the peptidoglycan backbone is rich in carboxylate groups, and the associated teichoic acids are rich in phosphate groups [17].

Fig. 5(a) shows that FTIR spectra of metal ions-free *A. protophormiae* biomass. The FTIR spectra clearly

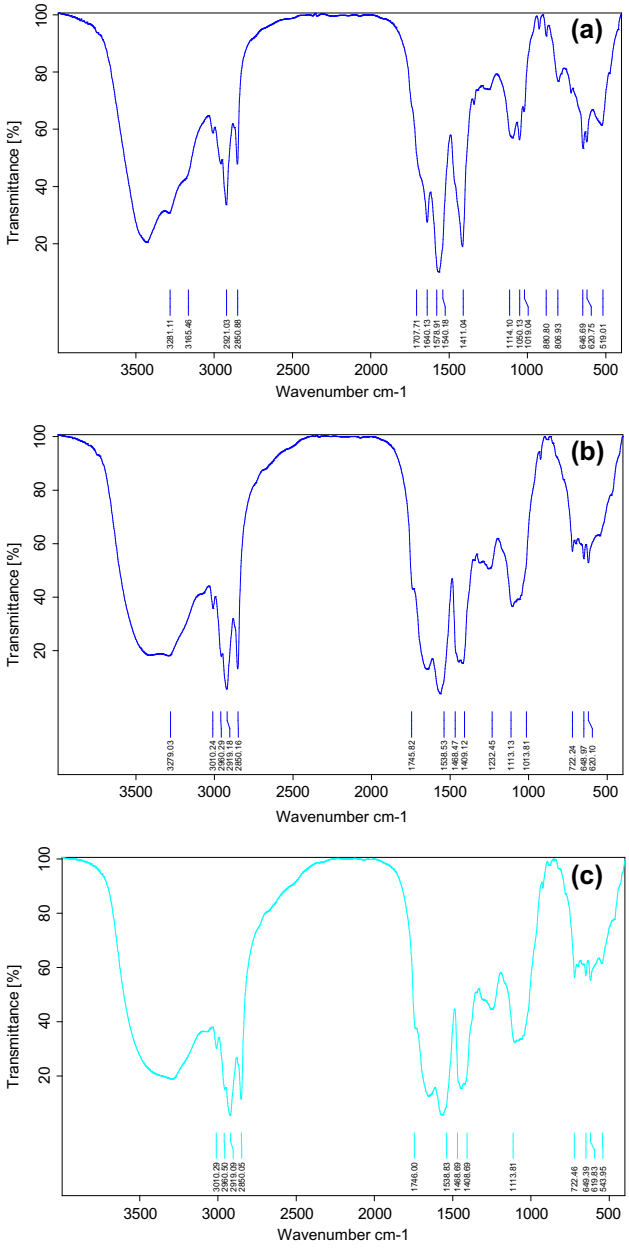

Fig. 5. FTIR spectra of before and after metal ions exposure to *A. protophormiae* biomass: (a) free of metal ions, (b) Cd-loaded, and (c) Pb-loaded.

demonstrate that different functional groups are present on the biomass. The large band around 3,280 cm^{-1} is commonly attributed to water [23]. In the range of 3,000–2,800 cm^{-1}, the bands are representative of symmetric and asymmetric vibrations of stretching of $–CH_3$ and $–CH_2$ groups. A peak observed at 1,707 cm^{-1} was attributed to carbonyl stretching in carboxylate groups or ester groups. A band located around 1,640 cm^{-1} may correspond to the superimposition of different Amide I band and a peak around 1,540 cm^{-1} corresponds to Amide II band. Around 1,411 cm^{-1}, $–CH_2$ bending vibration was observed. The peak around 1,114 cm^{-1} corresponds to the vibrations of C–O–P and/or P–O–P groups and the band around 1,050 cm^{-1} corresponds to the C–O and/or C–O–C from polysaccharides.

The Cd(II) adsorption induced some small modifications of the IR spectra (Fig. 5(b)). The neo-formed absorption peaks at 1,232 cm^{-1} clearly indicates the weakening of the P=O character as a result of Cd(II) binding to the phosphates [24]. A prominent change in peak positions in between 1,100 and 1,000 cm^{-1} for Cd(II) loaded biomass strongly suggest the involvement of carboxyl groups in Cd(II) uptake [24]. The overall spectral analysis strongly supports the major role of carboxyl and phosphate groups in Cd(II) binding by the bacterial biomass. A previous report on EXAFS analysis of the Cd(II) bound to the bacterial surface indicated that Cd(II) is coordinated by phosphate groups in a monodentate mode and by carboxyl groups in a bidentate fashion [25].

On the other hand, the HSAB theory on hard or soft acids and bases establishes that hard acids prefer to co-ordinate to hard bases and soft acids to soft bases. It should be stressed that although Cd^{2+} has been termed a soft metal in accordance with the classification of Pearson [26,27]; however, in fact, Cd^{2+} is regarded a borderline ion as a result of the lower product of its electro-negativity and ionic radius [28,29]. Accordingly, Cd(II) can readily bind with these O-containing functional groups present on the biomass. Similar results were obtained by Cd(II) adsorption by *A. protophormiae* biomass (Fig. 5(c)).

3.5.2. SEM-EDX

The biomass surface, before and after metal ion exposure, was characterized using SEM-EDX (Fig. 6). The SEM result shows that the biomass loaded with metal ions was markedly different from those free of metal ions, indicating that the metal ions adsorption induced substantial modifications on the surface.

Conclusive identification of the element was achieved by energy dispersive X-ray microanalysis (EDX). The EDX spectrum of the intact biomass (Fig. 6(a)) exhibited peaks of C, O, Al, Ca, P, Cl, Na, Mg, and S, indicating the presence of these elements in the biomass. After exposure to metal ions, the spectra (Fig. 6(b) and (c)) showed distinct Pb or Cd peaks, indicating the presence of both metals on the surface of the biomass (0.22 and 0.02 At.% for Cd and Pb, respectively). The atomic percent of P significantly increased after exposure to both Pb and Cd ions, presumably indicating the interaction between metal ions and

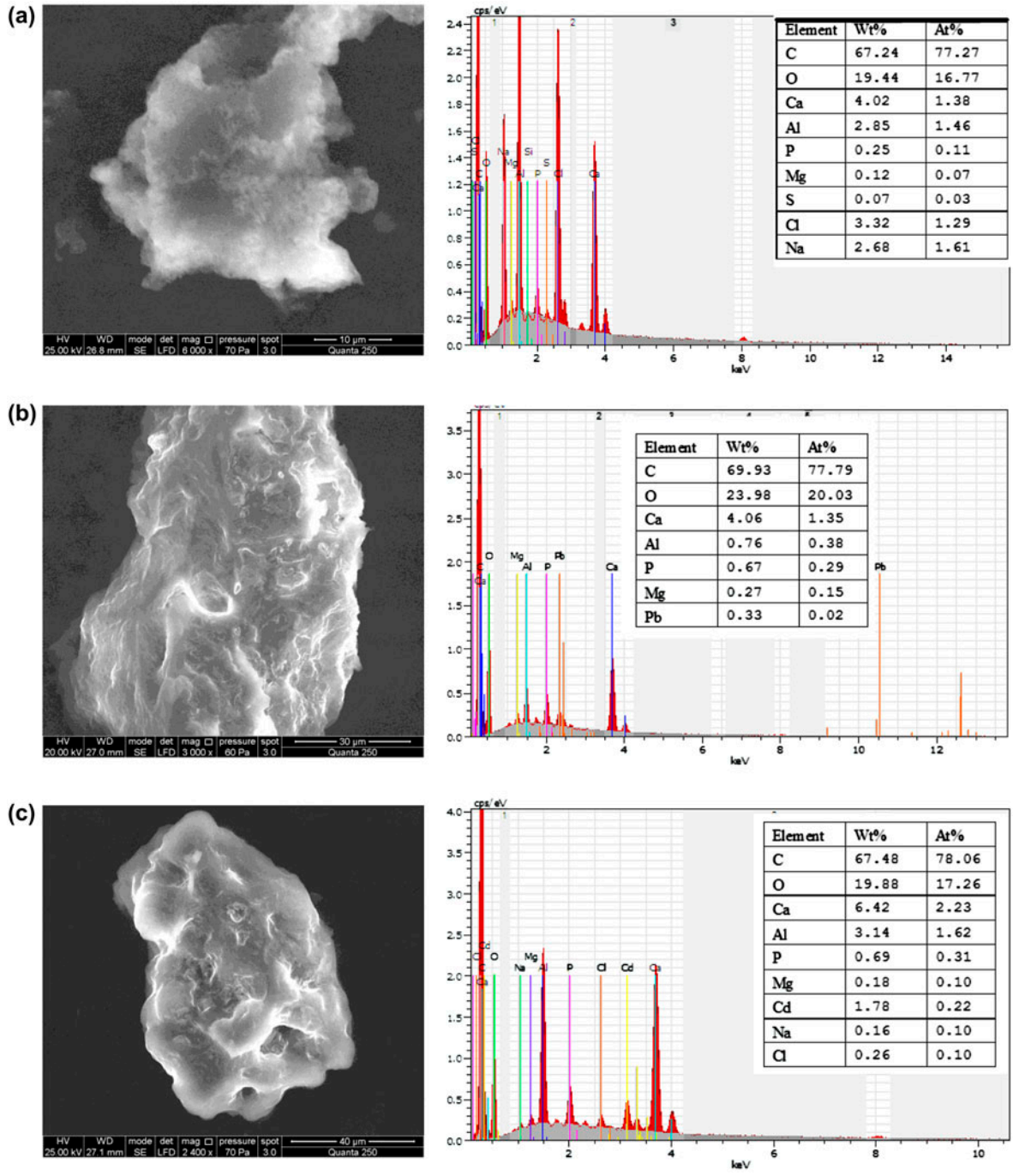

Fig. 6. SEM–EDS images of the intact and metal-loaded biomass: (a) biomass free of metal ions, (b) Cd-loaded biomass, and (c) Pb-loaded biomass. The inset is the elemental content.

P-containing functional groups (phosphate and/or-phosphoryl groups) on the surface of the biomass. The atomic percent of Pb was much less than that of Cd, suggesting Pb(II) removal was not totally by adsorption on to the biomass, but principally by precipitation as a consequence of an increase in solution pH.

3.5.3. AFM

The AFM is an ideal tool for determining changes in cellular morphology [30,31]. In the present study, AFM was used to investigate the bacterial cell surface morphology. Fig. 7 presents the morphological

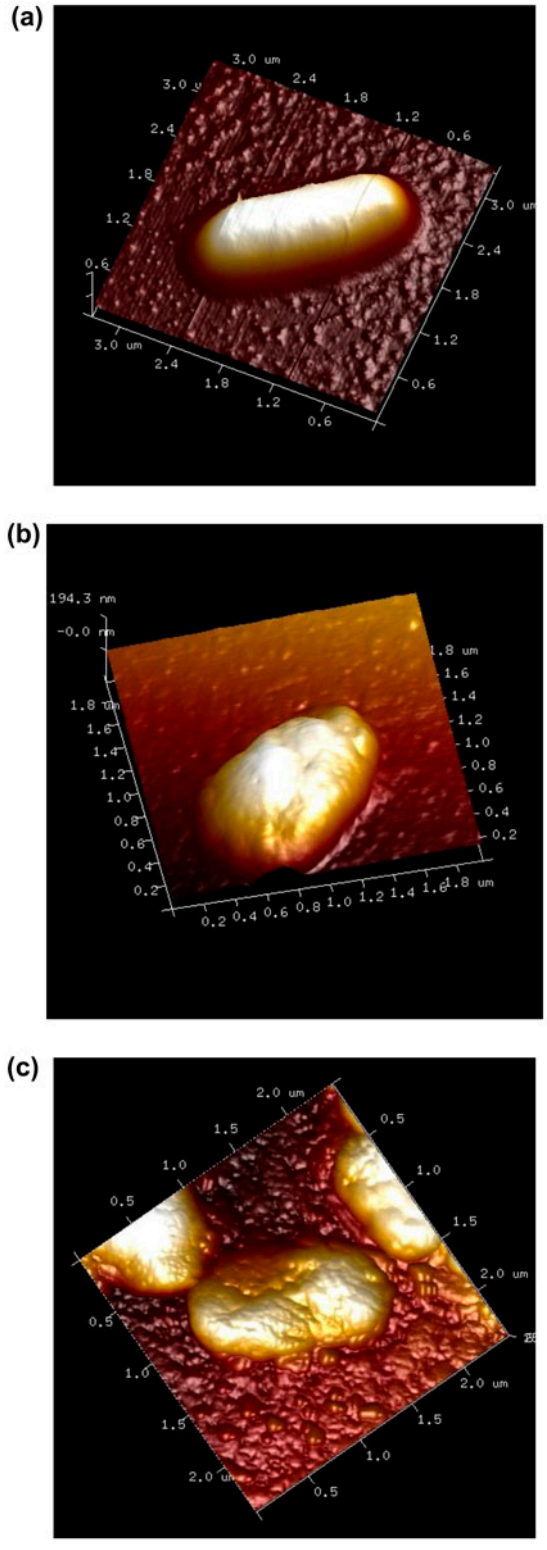

Fig. 7. AFM microscopic three-dimensional images of bacterial cells before and after metal ions exposure: (a) free of metal ions, (b) Cd-loaded, and (c) Pb-loaded.

comparison among the cells before and after both metal ions exposure. Overall results indicate that exposure of Pb or Cd to the biomass induced substantial modification on cell surfaces. The morphological distortion of the *A. protophormiae* cell on the surface of mica sheet enlarged after metal ions exposure is likely ascribed to the fact that the interaction of metal ions with surface functional groups leads to a change in surface architecture as reflected by an increase in surface roughness or irregularity. Another reason of increased roughness is possible rupturing of the bacterial cell following metal ion accumulation, which was reported by earlier workers characterizing *S. cerevisiae* following Pb(II) enrichment by AFM [32]. These phenomena might be caused by the release of light metal ions (Na^+, Mg^{2+}, Ca^{2+}, etc.), which is an important factor for the maintenance of osmotic tolerance.

4. Conclusions

The results of present studies show that *A. protophormiae* biomass was an efficient biosorbent of Pb(II) and Cd(II) ions in a dilute solutions. The main conclusions can be drawn as follows:

(1) Involvement of cellular phosphate and carboxyl functional groups in Cd(II) binding was evident from FTIR and SEM/EDX analyses. AFM showed substantial modification of bacterial cells after metal exposure to the biomass.
(2) Pb(II) was removed by both metal adsorption and precipitation, due to the pH shift that occurred during the process, while Cd(II) removal showed to be completely dependent of this pH shift.
(3) The presence of Pb(II) or Cd(II) in the medium promoted the release of Ca^{2+} but had a small influence on the release of Na^+ and Mg^{2+}.

Acknowledgments

The material is based upon work supported by Open-end Funds of Jiangsu Key Laboratory of Marine Biotechnology, Huaihai Institute of Technology (2011HS004).

References

[1] X.S. Wang, L.P. Huang, Y. Li, J. Chen, Removal of copper(II) ions from aqueous solution using *Sphingomonas paucimobolis* biomass, Adsorpt. Sci. Technol. 28 (2010) 137–147.

[2] X.S. Wang, Z.Z. Li, S.R. Tao, Removal of chromium (VI) from aqueous solution using walnut hull, J. Environ. Manage. 90 (2009) 721–729.
[3] X.S. Wang, H.H. Miao, W. He, H.L. Shen, Competitive adsorption of Pb(II), Cu(II), and Cd(II) ions on wheat-residue derived black carbon, J. Chem. Eng. Data 56 (2011) 444–449.
[4] K.S. Rao, M. Mohapatra, S. Anand, P. Venkateswarlu, Review on cadmium removal from aqueous solutions, Int. J. Eng. Sci. Technol. 2 (2010) 81–103.
[5] M. Danish, R. Hashim, M. Rafatullah, O. Sulaiman, A. Ahmad, Adsorption of Pb(II) ions from aqueous solutions by date bead carbon activated with $ZnCl_2$, Clean—Soil Air Water 39 (2011) 392–399.
[6] B. Özkahraman, I. Acar, S. Emik, Removal of Cu^{2+} and Pb^{2+} ions using CMC based thermoresponsive nanocomposite hydrogel, Clean—Soil Air Water 39 (2011) 658–664.
[7] J. Wang, C. Chen, Biosorbents for heavy metals removal and their future, Biotechnol. Adv. 27 (2009) 195–226.
[8] K. Vijayaraghavan, Y.S. Yun, Bacterial biosorbents and biosorption, Biotechnol. Adv. 26 (2008) 266–291.
[9] F.M. Morsy, S.H.A. Hassan, M. Koutb, Biosorption of Cd(II) and Zn(II) by nostoc commune : Isotherm and kinetics studies, Clean—Soil Air Water 39 (2011) 680–687.
[10] S. Murugavelh, K. Mohanty, Bioreduction of Hexavalent chromium by live and active *Phanerochaete chrysosporium*: Kinetics and modeling, Clean—Soil Air Water 40 (2012) 746–751.
[11] B.J. Seh-Bardan, R. Othman, S.A. Wahid, A. Husin, F. Sadegh-Zadeh, Column bioleaching of arsenic and heavy metals from gold mine tailings by *Aspergillus fumigatus*, Clean—Soil Air Water 40 (2012) 607–614.
[12] M.Z. Alam, S. Ahmad, Chromium removal through biosorption and bioaccumulation by bacteria from tannery effluents contaminated soil, Clean—Soil Air Water 39 (2011) 226–237.
[13] S.A. Jabasingh, G. Pavithra, response surface approach for the biosorption of Cr^{6+} ions by *Mucor racemosus*, Clean—Soil Air Water 38 (2010) 492–499.
[14] J.H. Suh, J.W. Yun, D.S. Kim, Cation (K^+, Mg^{2+}, Ca^{2+}) exchange in Pb^{2+} accumulation by *Saccharomyces cerevisiae*, Bioprocess Eng. 21 (1999) 383–387.
[15] G.M. Gadd, Interactions of fungip with toxic metals, New Phytol. 124 (1993) 25–60.
[16] L.M. He, B.M. Tebo, Surface Charge properties of and Cu(II) adsorption by spores of the marine *Bacillus* sp. strain SG-1, Appl. Environ. Microbiol. 64 (1998) 1123–1129.
[17] Q.F. Zhou, Microbiology of Environmental Engineering, Higher Education Press, China, Beijing, 1998.
[18] S.K. Kazy, S.F. D'Souza, P. Sar, Uranium and thorium sequestration by a *Pseudomonas* sp.: Mechanism and chemical characterization, J. Hazard. Mater. 163 (2009) 65–72.
[19] C. Chen, J.L. Wang, Cation (K^+, Na^+, Ca^{2+}, Mg^{2+}) release in Zn (II) biosorption by *Saccharomyces cerevisiae*, Environ. Sci. 27 (2006) 2261–2267 (in chinese).
[20] M. Tsezos, E. Remoudaki, V. Angelatou, A systematic study on equilibrium and kinetics of biosorptive accumulation. The case of Ag and Ni, Int. Biodeterior. Biodegrad. 35 (1995) 129–153.
[21] P.A.S.S. Marques, M.F. Rosa, H.M. Pinheiro, H^+ effects on the removal of Cu^{2+}, Cd^{2+}, Pb^{2+} from aqueous solution by waste brewery biomass, Bioprocess Eng. 23 (2000) 135–141.
[22] R.D. Shannon, C.T. Prewitt, Revised values of effective ionic radii, Acta Crystallogr., Sect. B: Struct. Crystallogr. Cryst. Chem. 26 (1970) 1046–1048.
[23] J. Bayo, G. Esteban, J. Castillo, the use of native and protonated grapefruit biomass (*Citrus paradisi* L.) for cadmium(II) biosorption: Equilibrium and kinetic modelling, Environ. Technol. 33 (2012) 761–772.
[24] S.K. Kazy, S.K. Das, P. Sar, Lanthanum biosorption by a *Pseudomonas* sp.: Equilibrium studies and chemical characterization, J. Ind. Microbiol. Biotechnol. 33 (2006) 773–783.
[25] K.M. Kemner, E.J. O'Loughlin, S.D. Kelly, M.I. Boyanov, Synchrotron X-ray investigations of mineral-microbe-metal interactions, Elements 1 (2005) 217–221.
[26] R.G. Pearson, Hard and soft acids and bases, J. Am. Chem. Soc. 85 (1963) 3533–3539.
[27] R.G. Pearson, Chemical hardness and bond dissociation energies, J. Am. Chem. Soc. 110 (1988) 7648–7690.
[28] E. Nieboer, D.H.S. Richardson, The replacement of the nondescript term 'heavy metals' by a biologically and chemically significant classification of metal ions, Environ. Pollut. Series B, Chem. Phys. 1 (1980) 3–26.
[29] A. Alfarra, E. Frackowiak, F. Béguin, The HSAB concept as a means to interpret the adsorption of metal ions onto activated carbons, Appl. Surf. Sci. 228 (2004) 84–92.
[30] S.K. Kazy, S.F. D'Souza, P. Sar, Uranium and thorium sequestration by a *Pseudomonas* sp.: Mechanism and chemical characterization, J. Hazard. Mater. 163 (2009) 65–72.
[31] X.S. Wang, Cd (II) removal by marine *Arthrobacter protophormiae* biomass: Mechanism characterization and adsorption performance, Desalin. Water Treat. 51 (40–42) (2013) 7710–7720.
[32] C. Chen, J.L. Wang, Cell surface characteristics of *Saccharomyces cerevisiae* after Pb (II) uptake, Acta Sci. Circumstant. 31 (2009) 1587–1593.